Journal of NUCLEAR SCIENCE and TECHNOLOGY, Supplement 1, p. 530–534 (March 2000)

# Systematic Comparisons of Measurements and EGS4 Regarding 20-40 keV Photons

Yoshihito NAMITO[*1,†], Syuichi BAN[*1], Hideo HIRAYAMA[*1], Nobuteru NARIYAMA[*2], Hiroshi NAKASHIMA[*3], Yoshihiro NAKANE[*3] and Syun-ichi TANAKA[*3]

[*1] *High Energy Accelerator Research Organization (KEK)*
[*2] *Ship Research Institute*
[*3] *Japan Atomic Energy Research Institute*

To investigate the validity of the EGS4 code regarding photon transport in the keV region, we performed systematic comparisons of measurements and EGS4. The scattered-energy spectra of monochronized synchrotron-radiation photons toward 90° by samples (C, Cu, Pb) were measured using high-purity Ge detectors. The incident photons were in a linearly polarized beam of 20, 30 and 40 keV. EGS4 calculations were performed in default status and with improvements of low-energy photon transport (linearly polarized photon scattering, Doppler broadening, L-X and K-X). The measurement and calculations were compared in absolute values. Both the intensity and the shape of the peaks were compared. EGS4 calculations with improvements in low-energy photon transport agreed well with the measurements.

***KEYWORDS: Monte Carlo, calculation, EGS4, keV, photons, scattering, benchmark, experiment, synchrotron radiation, Compton scattering, Rayleigh scattering, K-X ray, L-X ray***

## I. Introduction

Expansion of the general-purpose electron-photon Monte-Carlo transport code EGS4 [(1)] is being continued. One subject concerning the expansion is a detailed treatment of photon transport in the keV region. The purpose of this comparison is to verify the validity of the EGS4 code in this energy region.

Measurements of 20-40 keV photon transport were performed using monochronized synchrotron-radiation. The merits of monochronized synchrotron-radiation is the use of mono-energy and mono-direction photons. This experiment is free from scattering inside the source or by the source holder, which is inevitable in any experiment using a radio-isotope source. Thus, this experiment is performed under much more clear conditions compared to an experiment using a radio-isotope source. Also, the geometry is simple and well defined. The measurement value is given in absolute values. Thus, this experimental-data may be useful as a benchmark in a few ten keV region to examine the validity of a photon transport code.

The Rayleigh scattered, Compton-scattered, multiply scattered photons, and fluorescent photons (K- and L-X rays) are included in the photon spectra. The scattering is influenced by the photon linear polarization, and the Compton scattering is influenced by electron binding and Doppler broadening. By simulating this experiment, it is possible to check the calculation program regarding these points.

[*1] *Oho, Tsukuba, Ibaraki 305-0801*
[*2] *Shinkawa, Mitaka, Tokyo 181-0004*
[*3] *Tokai-mura, Ibaraki 319-1195*
[†] Corresponding author, Tel. +81-298-64-1993, Fax.+81-298-64-1993, E-mail: yoshihito.namito@kek.jp

## II. Measurement

### 1. Experimental details

The measurement was performed at a BL-14C in the 2.5-GeV synchrotron-light facility (KEK-PF). The experimental arrangement is shown in **Fig. 1**. Photons from a vertical wiggler were used after being monochronized by a Si(1,1,1) double-crystal monochromator. The incident beams were 20, 30 and 40 keV linearly polarized photons. The polarization vector was in the vertical direction and the degree of linear polarization ($P$) is shown in **Table 1**. Depending on the detune of the monochrometer, $P$ is subject to change by a few %.

In Fig. 1, the propagation and polarization vectors of an incident photon are shown as $\vec{k_0}$ and $\vec{e_0}$. Incident photons passed through a collimator ($C_0$) with an opening diameter($D_0$) of 2 mm and a free air ionization chamber (FAIC), and were scattered by the sample (S). The photon intensity was monitored by the FAIC, which was calibrated by a calorimeter.[(2)] After passing an air layer and Kapton film, photons entered the vacuum chamber (VC). The thickness of air and Kapton is summarized in **Table 2**.

A list of the samples and their thickness is given in **Table 3**. The normal vector of the samples was $(-\cos\xi\sin\eta, -\sin\xi, \cos\xi\cos\eta)$. While the design value of $\xi$ and $\eta$ was 45° and 45°, the actual value of $\xi$ and $\eta$ was 45.88° and 45°. Thus, the actual value of the normal vector was (–0.492, –0.718, 0.492). The effective thickness for incident photons of the Cu and Pb samples were more than 10 mean-free-paths for all of the photon energies used; these samples could be treated as infinitely

thick samples. The samples were contained in a vacuum chamber, and vacuum pipes were placed between the vacuum chamber and the Ge detectors in order to reduce any scattering due to air.

Photons through collimators ($C_1$ and $C_2$) located in the X and Y directions were detected by Ge detectors (Ge-1 and Ge-2). Before entering Ge detectors, photons pass through Kapton film and air layer. The distances from the surface of the sample to the exits of the collimators ($L_1$ and $L_2$) were 424 and 436 mm, respectively, and the opening diameters of the collimators ($D_1$ and $D_2$) were 5.01 and 5.04 mm, respectively. The scattered photon intensity had an azimuth angle dependence, since the incident photon beam comprized linearly polarized photons. To observe the effect of linear polarization, the scattered-photon intensity was measured by two Ge detectors located in two different azimuth-angle directions. Two high-purity Ge low-energy-photon detectors (ORTEC GLP16195/10 and GLP16195/10P) were used for the measurement; the former and the later were used as Ge-1 and Ge-2, respectively. The absorbing layers of Ge detectors are summarized in **Table 4** [3].

The signal from the detector was amplified by an ORTEC 572 amplifier, passed through a 1850-ADC(Seiko EG&G) and stored in 4k-memory in a Model-7800 multichannel analyzer (Seiko EG&G). The typical accumulation time was 600 sec.

### 2. Data analysis

An energy calibration of the measured counts of scattered photon was performed. The $L_\alpha$ ($L_{\alpha_1}$+$L_{\alpha_2}$) peak of Pb and $K_{\alpha_1}$ peak of Pb was used for the energy calibration. The $K_{\alpha_1}$ of Pb was emitted due to the photoelectric effect of higher harmonic incident photons from the monochrometer.

Based on the measured counts of scattered photons ($n_x(k)$ and $n_y(k)$), the photon counts per incident photon per solid angle toward the $x$ and $y$ directions ($C_x$ and $C_y$) were derived as

$$C_x(k) = \frac{1}{\Omega_x}\left(\frac{n_x(k)}{I_0} - \frac{n_x^{bg}(k)}{I_0^{bg}}\right), \quad (1)$$

$$C_y(k) = \frac{1}{\Omega_y}\left(\frac{n_y(k)}{I_0} - \frac{n_y^{bg}(k)}{I_0^{bg}}\right). \quad (2)$$

Here, $k$ is the scattered photon energy, $\Omega_x$ and $\Omega_y$ are the opening solid angles of the collimators, and $n_x^{bg}$ and $n_y^{bg}$ are the background counts obtained from a no-sample run. The background count was negligibly small (< 0.2% of sample run). $I_0$ and $I_0^{bg}$ are the number of incident photons during a sample run and a no-sample run. The attenuation of incident photons due to air and Kapton film between FAIC and VC was considered when $I_0$ and $I_0^{bg}$ were calculated. A dead-time correction was made using the ratio of the live time and the real time of ADC. The dead time was controlled to be less than 2%. Correction for pile up is not considered here. The pile up was controlled to be less than 1%.

The statistical error is shown in the figures and is not included here. The major sources of errors are the monitor (1.4%), the orientation of the sample (1%), the solid angle of collimators (1%), and $P$ (2%). The error in $P$ strongly affects $C_y(k)$, because they are proportional to $(1-P)$, and $P$ is about 0.8. In total, the errors of $C_x(k)$ and $C_y(k)$ are estimated to be about 3% and 10%, respectively ($1\sigma$).

The fluctuation of the measured value is about the same as these estimated errors, except for Rayleigh scattered photons.

Measurement were performed for 9 conditions (3 samples times 3 energies). The measured photon spectra for an incident energy of 40 keV are shown in **Figs. 3** to **6**.

## III. EGS4 Calculation

### 1. Improvement

The EGS4 code with the low-energy photon transport expansion developed at KEK was used. In addition to the physical processes in the standard EGS4 code, we considered the following physical processes in the calculation;

1. Effect of linear polarization on Compton and Rayleigh scattering. [4, 6]
2. Doppler broadening of a Compton-scattered photon. [5, 6]
3. Up to 10 K-X rays is considered.
4. L-X rays. Some of the authors (HH, YN and SB) released a preliminary version program to treat L-X rays in EGS4 [7]. After that, the following improvements of the physical model were made:
   (a) The energy dependence of the subshell ionization cross sections ($L_{\rm I}$, $L_{\rm II}$ and $L_{\rm III}$) is treated by approximately treating the cross sections in a log-log fitting. The agreement of measured and calculated L-X rays from $L_{\rm I}$ (ex. $L_\gamma$ ) was apparently improved by this treatment.
   (b) Experimental L relative x-ray emission rates, summarized by Salem et al,[8] were used. Theoretical L relative x-ray emission rates, calculated by Scofield,[9] were used for L-X rays which ref.[8] did not mention. We did not use the L-X relative x-ray emission rates in Ref.[10].
   (c) The photon cross section and branching ratio in an energy bin which contains K- or L-edge is determined using the extrapolation from higher or lower energy bin.

In the calculation, we ignored the following points, which may have some effect on the measurement:

1. Interference of Rayleigh scattering.
2. Interference of Compton-scattered photons.[11]

This last phenomenon has not yet been studied well.

**Table 1** Source conditions

| Energy (keV) | 40 | 30 | 20 |
|---|---|---|---|
| Linear polarization $P$ | 0.85 | 0.83 | 0.82 |
| Energy width $\Delta E/E$ | | $10^{-3}$ | |
| Intensity ($\gamma$/sec/cm$^2$) | | $10^{11}$ | |

**Table 2** Thickness of the absorbing layer in measurements for element samples.

| Place | Kapton (g/cm$^2$) | Air (cm) |
|---|---|---|
| FAIC–VC | $3.58\times10^{-3}$ | 8.7* |
| VC–Ge-1 | $3.58\times10^{-3}$ | 3.5 |
| VC–Ge-2 | $3.58\times10^{-3}$ | 5.0 |

* Between the center of FAIC and Kapton film

**Table 3** Thickness of the samples (in g/cm$^2$)

| C | Cu | Pb |
|---|---|---|
| 0.1325 | 1.79 | 0.568 |

**Table 4** Absorbing layers of the Ge detector

| | Be (mm) | Inactive Ge ($\mu$m) |
|---|---|---|
| GLP-16195/10 | 0.5 | ~0.3 |
| GLP-16195/10P | 0.127 | ~0.3 |

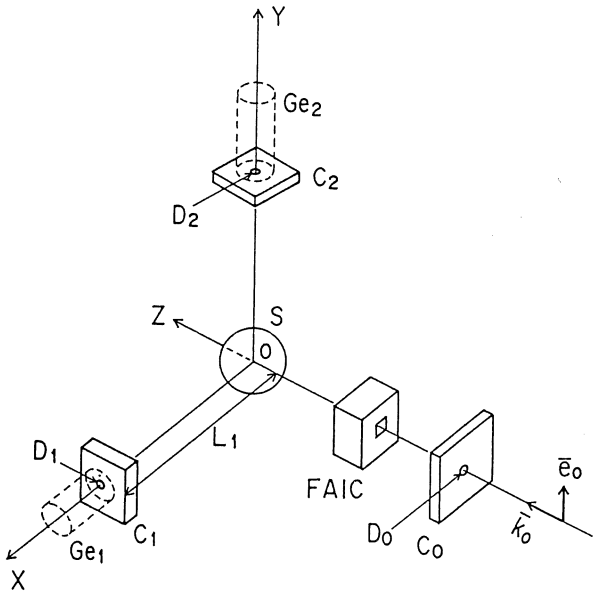


**Fig. 1** Experimental arrangement

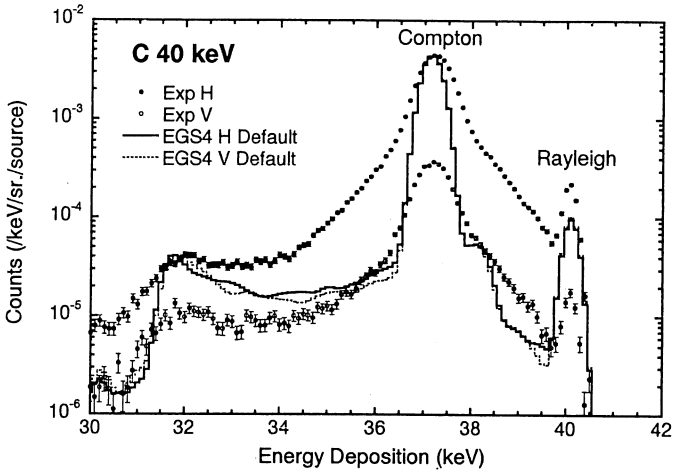


**Fig. 2** Photons from a C target. Incident energy, $k_0$=40 keV. "Default" means the EGS4 code without any low-energy photon-transport expansion. The calculated values are Gauss-smeared with $\sigma$=0.35 keV.

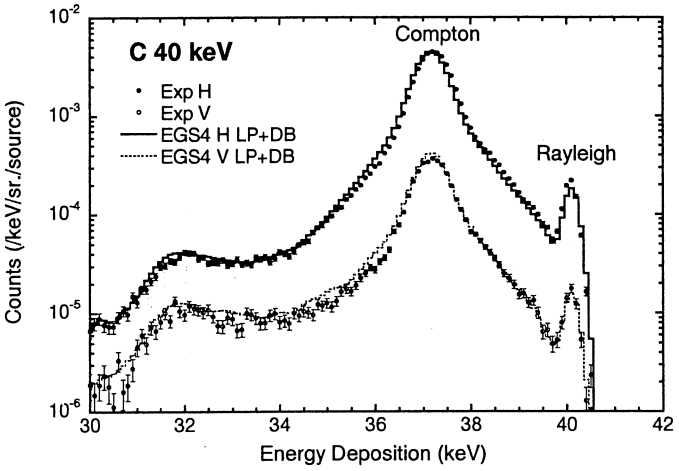


**Fig. 3** Photons from a C target. The incident energy, $k_0$=40 keV. LP+DB means that linearly polarized photon scattering and Doppler broadening were considered in the calculation. The calculated values are Gauss-smeared with $\sigma$=0.35 keV.

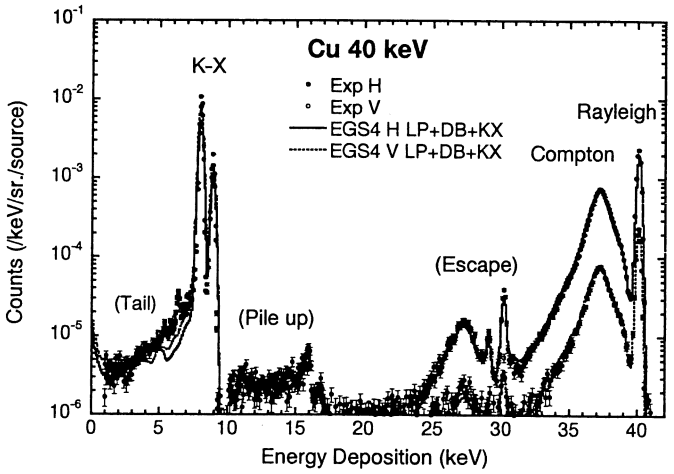


**Fig. 4** Photons from a Cu target. See the caption of Fig.3 concerning the measurement and calculation conditions.

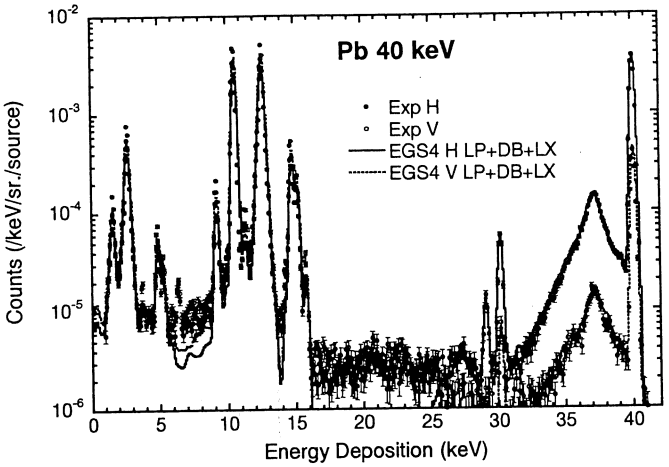


**Fig. 5** Photons from a Pb target. LX means that the L-X ray was considered in the calculation. See the caption of Fig.3 concerning the measurement and calculation condition.

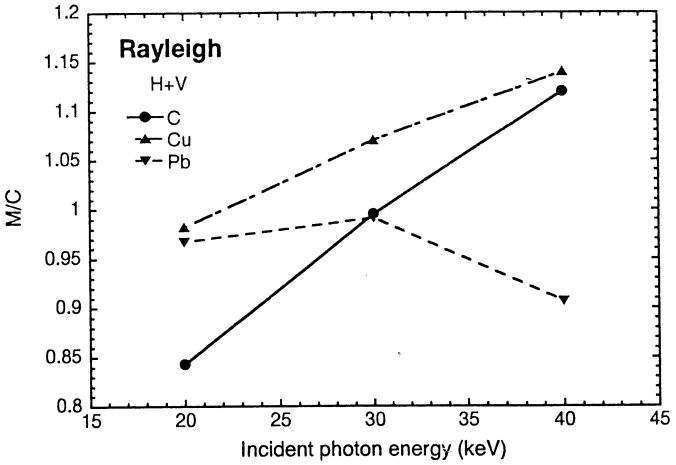


**Fig. 8** Ratio of the measured and computed intensity of the Rayleigh-scattered photons.

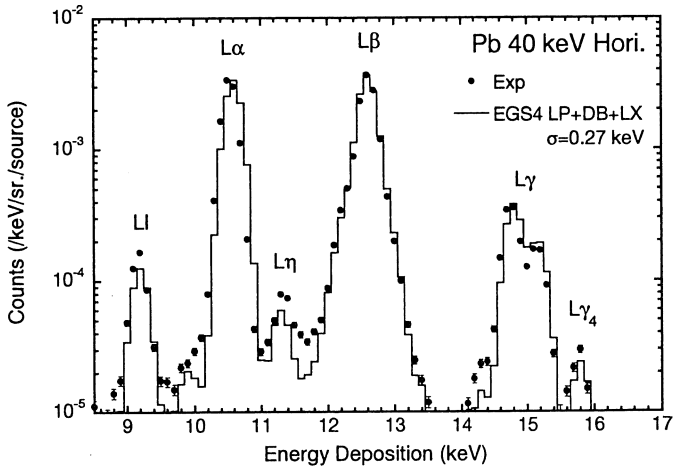


**Fig. 6** L-X photons from a Pb target. $k_0$=40 keV. The calculated values are Gauss-smeared with $\sigma$=0.27 keV.

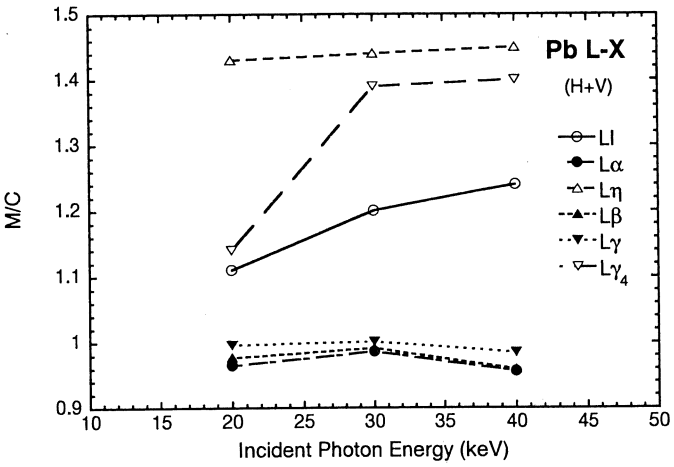


**Fig. 9** Ratio of the measured and computed intensity of L-X rays.

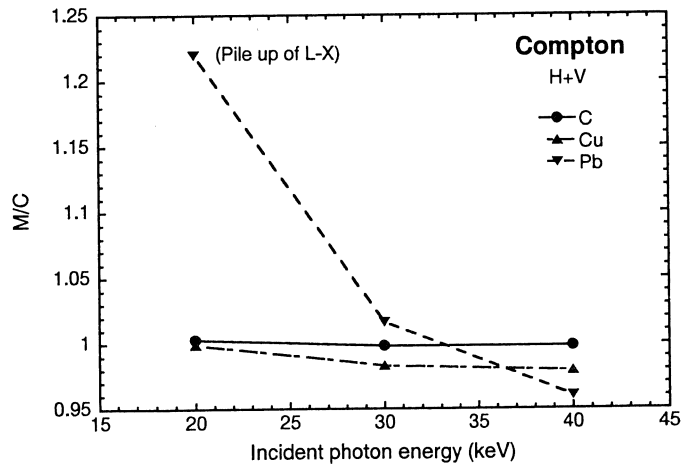


**Fig. 7** Ratio of the measured and computed intensity of Compton-scattered photons. H+V means that the sum of the horizontal and vertical components was compared.

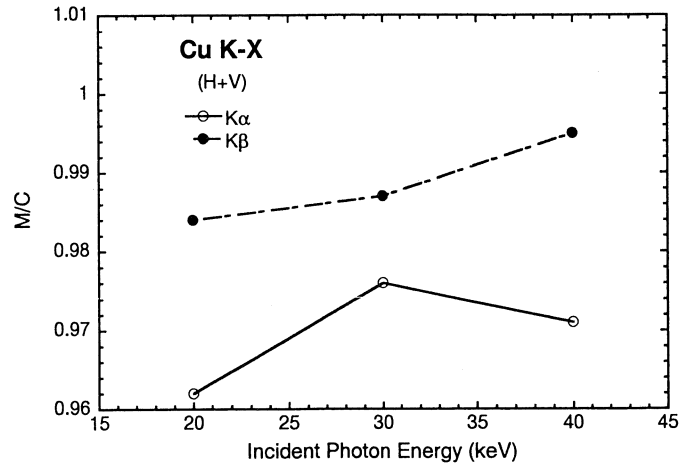


**Fig. 10** Ratio of the measured and computed intensity of the K-X rays.

### 2. Two-step calculation

The calculation was divided into two steps. In the first step, photon transport inside the sample was performed and scattered photons toward 90° were scored. In the second step, photon transport inside the Ge detector was performed using the scattered photon spectra obtained in the first step as an incident photons. The energy deposition in the Ge region was scored and compared with measured pulse height spectra.

An EGS4 calculation without any low-energy photon transport expansion is shown in **Fig. 2**. An EGS4 calculation with a low-energy photon transport expansion is shown in Figs. 3-6.

## IV. Comparison

A comparison of the measured and calculated photon spectra for 40 keV incident photons is shown in Figs. 3 to 6. The ratio of the measured and computed intensity of Compton-scattered, Rayleigh-scattered, L-X ray and K-X ray are shown in **Figs. 7** to **10**.

The result of comparisons of the measurement and EGS4 calculations was as follows:

1. Compton scattering: Both the intensity and spectra agreed well.
2. Rayleigh scattering: Agreed reasonably well. In some cases, C/M reaches 0.8 or 1.2. This was due to interference. This was verified by observing the interference pattern using an imaging plate.
3. Multiple scattering: Agreed well.
4. L-X rays: Major 3 L-X rays agreed well. Other 3 L-X rays differs up to 50%.
5. K-X : Agreed well.

## V. Discussion

The experimental data will be provided in printed form [12] as well as on the WWW. Both the energy-deposition data and the photon spectra will be included.

—REFERENCES—


(1) Nelson, W. R., Hirayama, H., Rogers, D. W. O. : *SLAC-265* (Stanford University, Stanford, 1985).
(2) Nakashima, H., Tanaka, S., Yoshizawa, M., Hirayama, H., Ban, S., Namito, Y., Nariyama, N. : *Nucl. Instrum. and Meth.*, **A310**, 696 (1991).
(3) "Solid-State Photon Detector Operators Manual" (EG&G ORTEC).
(4) Namito, Y., Ban, S., Hirayama, H. : *Nucl. Instr. Meth.*, **A332**, 277 (1993).
(5) Namito, Y., Ban, S., Hirayama, H. : *Nucl. Instr. Meth.*, **A349**, 489 (1994).
(6) Namito, Y., Ban, S., Hirayama, H. : *KEK Internal*, **95-10** (1995).
(7) Hirayama, H., Namito, Y., Ban. S. : *KEK Internal*, **96-10** (1996).
(8) Salem, S. I., Panossian, S. L., Krause, R. A. : *Atomic Data and Nucl. Data Tables*, **14**, 91 (1974).
(9) Scofield, J. H. : *Atomic Data and Nucl. Data Tables*, **14**, 121 (1974).
(10) Firestone, R. B. : "*Table of Isotopes*", 8th ed., John Wiley & Sons, Inc. Table 7b-7d (1996).
(11) Schülke, W., Mourikis, S. : *Acta Cryst.*, **A42**, 86 (1986).
(12) Namito, Y., Ban, S., Hirayama, H. : "Low Energy Photon Transport Benchmark Problems", *KEK Report* (On Preparation).